Optimization of Noise Performance for Various Topologies of Planar Microwave Active Filters Using Noise Wave Techniques

Hilal Ezzedine, Laurent Billonnet, Bernard Jarry, *Senior Member, IEEE,* and Pierre Guillon, *Senior Member, IEEE*

***Abstract*—In this paper, two types of microwave active filters are studied. First we show how, using a noise wave formalism, the noise factor of three topologies of active recursive filters can be effectively minimized by using appropriate unbalanced power dividers/combiners and an amplifier. A comparison between the different topologies is given. Simulations and practical results are presented and validate our approach. In a second part, the noise wave formalism is applied to $\lambda/2$ microstrip active filters. We show how the appropriate choice of coupling between lines and resonators can achieve low-noise filters. Simulations and practical results are also presented.**

***Index Terms*—Active filters, low noise, noise wave formalism, planar technology, recursive filters.**

I. Introduction

WHEN introducing active devices in microwave filters, new parameters must be taken into account as compared to microwave passive filters [2]. Some of these parameters are the electrical and thermal stabilities, the circuit noise performance, the power handling behavior in general, and the dissipated power.

In this article we use a noise wave formalism to analytically evaluate noise figures of different types of microwave active filters. The objective here is to minimize the noise figure of each circuit to find the best topologies and structures in terms of noise performance. Two types of active filters are analytically studied, simulated, and measured:

We first focus on recursive planar microwave active filters. For this type of filter, three topologies are studied. For each topology, we determine the values of the input and output couplings and of the gain needed to obtain a given transfer function and the minimum corresponding noise factor.

We then study $\lambda/2$ microstrip planar filters whose losses are compensated by a feedback amplifier-based loop. In this case, we find the appropriate coupling values between the amplifier line section and the resonator to obtain the minimum noise factor. We illustrate our methodology with the simulated and experimental results proving that the appropriate choice of the couplings can achieve low-noise bandpass filters while maintaining the same transfer function performances.

Manuscript received March 30, 1998; revised September 2, 1998.

The authors are with the Institut de Recherche en Communications Optiques et Microondes, Université de Limoges, 87060 Limoges, France.

Publisher Item Identifier S 0018-9480(98)09239-4.

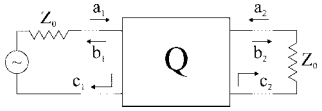

Fig. 1. Two-port circuit described by noise waves and scattering parameters.

II. Noise Wave Formalism [1]

This method consists of modeling the noise of a two-port device with internal noise wave generators c_1 and c_2 (see Fig. 1). These noise waves are time-varying complex correlated random variables characterized by a Hermitian matrix. Their contribution to the scattering waves b_1 and b_2 can be expressed in the following manner:

$$\begin{pmatrix} b_1 \\ b_2 \end{pmatrix} = \begin{pmatrix} S_{11} & S_{12} \\ S_{21} & S_{22} \end{pmatrix}_Q \begin{pmatrix} a_1 \\ a_2 \end{pmatrix} + \begin{pmatrix} c_1 \\ c_2 \end{pmatrix}.$$

The correlation matrix C_S is given by

$$C_S = \begin{pmatrix} \overline{|c_1|^2} & \overline{c_1 c_2^*} \\ \overline{c_2 c_1^*} & \overline{|c_2|^2} \end{pmatrix}$$

where the diagonal terms represent the 1-Hz bandwidth available noise power at the input and output ports. The off-diagonal terms are correlation products. The matrix components are referred to as noise wave parameters.

The two port noise figure is then defined as

$$F = \frac{P_S + P_Q}{P_Q} = 1 + \frac{P_S}{P_Q}$$

where

- P_S noise power at the output of the two-port Q due to the source impedance;
- P_Q noise power at the output of the two-port Q due to the quadripole Q.

We apply the noise wave technique to an ideal unilateral amplifier. Referring to Fig. 2, we obtain the noise factor F_A of the unilateral amplifier supposed to be matched to 50 Ω. We analytically obtain

$$F_A = 1 + \frac{\overline{|c_2|^2}}{|G b_g|^2} \Rightarrow \frac{\overline{c_2|^2}}{|b_g|^2} = (F_A - 1)|G|^2. \qquad (1)$$

In the next Section, we will use this last expression to calculate the noise factor of our filters as a function of the noise factor of the amplifier F_A.

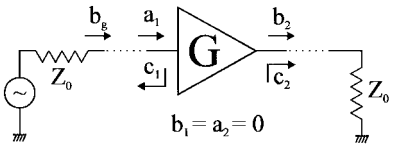

Fig. 2. Noise wave formalism applied to a unilateral amplifier matched to 50 Ω.

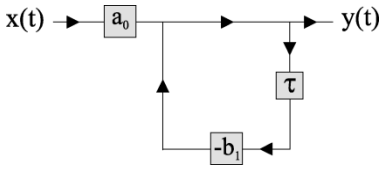

Fig. 3. Flowgraph of a first-order recursive filter.

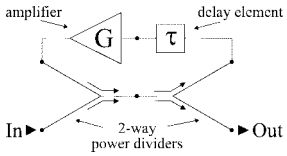

Fig. 4. Topology of a first-order filter at microwaves using blocks matched to 50 Ω.

III. First-Order Microwave Active Recursive Filters

Feasibility of first-order recursive filters, derived from digital low frequency concepts, is now well established both in hybrid and monolithic microwave integrated circuit (MMIC) technology [3]. Expression (2), where $x(t)$ $[y(t)]$ is the input [output] of the system, shows the time-domain equation of a first-order structure whose flowgraph is given in Fig. 3

$$y(t) = a_o x(t) - b_1 y(t-\tau). \tag{2}$$

The corresponding transfer function in the z-notation is given by (3) where $z = e^{-2j\pi f\tau}$

$$H(Z) = \frac{a_o}{(1 + b_1 z^{-1})}. \tag{3}$$

Preserving low frequency principles, implementation of the structure at microwaves is presented in Fig. 4 and requires three different blocks matched to 50 Ω: one delay component τ, an amplifier G as a weighting parameter, and two power dividers/combiners for the signal summation within the structure [3].

Recently, this first-order filter has been implemented [3], [4] on a 100-μm-thick GaAs substrate using a MMIC design process. Layout of the MMIC chip is presented in Fig. 5. A 3-dB power divider/combiner is used in association with an amplifier of gain value $G = 1.316$ (2.4 dB) providing the necessary b_1 value. Since noise performances were not considered during the different design steps, we clearly obtain a poor noise factor of 11.7 dB at the center frequency $f_o = 1/(2\tau) = 10$ GHz. The noise factor of the amplifier at the same frequency has been estimated at about 9.3 dB using a CAD software.

Fig. 6 presents the measured S_{21} parameter of the filter and the corresponding noise figure in the 8–12 GHz range.

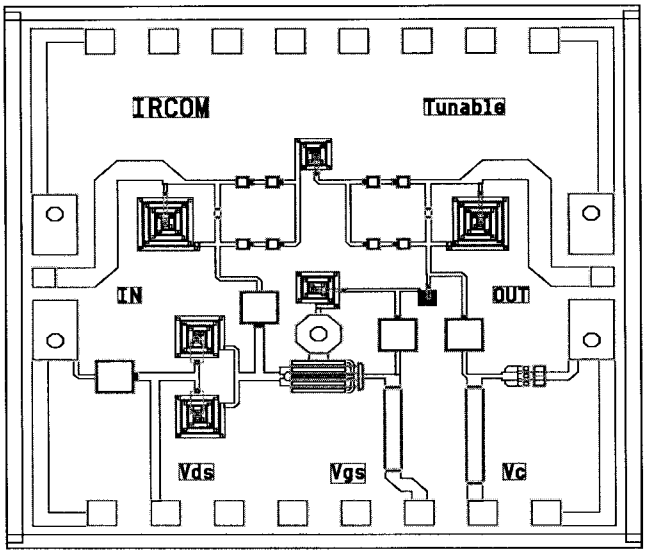

Fig. 5. Layout of the first-order active recursive filter (GaAs substrate 2 × 2 mm).

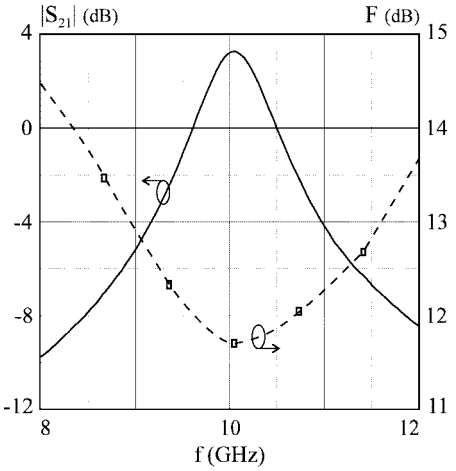

Fig. 6. Measured S_{21} and noise figure of a MMIC first-order recursive filter.

In fact, recursive response using the same concepts can be obtained thanks to different topologies in terms of the placement of the amplifier within the structure. So, the problem is now to know how to choose the correct gain value G, noise factor value F_A, and the two power dividers/combiners at the input and output of the filter, to obtain a given first-order response with a minimum noise factor at f_o for each topology. Then, we will be able to find out the best topology.

A. Different Topologies of Microwaves Active Recursive Filters

1) Topology 1: Amplifier Placed Within the Feedback Branch: The first topology is given in Fig. 7. Initially we suppose $G = G_o e^{-2j\pi f\tau}$ with G_o a positive real gain value and τ the delay-time of the filter. The transfer function of the filter is then given by

$$H_1(f) = \frac{\alpha_1\alpha_2}{1 - G\beta_1\beta_2}.$$

To calculate the noise powers P_S and P_Q using the noise wave formalism, we have to find the noise correlation matrix

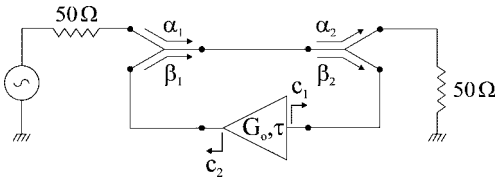

Fig. 7. Topology 1. Amplifier placed within the feedback branch.

of the circuit. To do this, the global circuit is first divided into active and passive subcircuits. Each of these elements is characterized by its own scattering matrix S and noise correlation matrix C_S. To find the complete circuit $S_{\rm net}$ and $C_{\rm net}$ matrices, we only have to solve the equations obtained by reconnecting the active and passive parts of the circuit [1]. The scattering matrix and the correlation matrix of the passive circuit are noted T and C_t (two power/divider circuits), respectively, and are given by

$$T = \begin{pmatrix} 0 & \alpha_1\alpha_2 & \alpha_1\beta_2 & 0 \\ \alpha_2\alpha_2 & 0 & 0 & \alpha_2\beta_2 \\ \alpha_1\beta_2 & 0 & 0 & \beta_1\beta_2 \\ 0 & \alpha_2\beta_1 & \beta_1\beta_2 & 0 \end{pmatrix}$$
$$C_t = KT(I - TT')$$

where T' indicates the transposed conjugate matrix of T, I is the identity matrix, T is the physical temperature of the device, and K is Boltzmann's constant.

The scattering matrix S and the correlation matrix C_S of the active circuit (unilateral amplifier matched to 50 Ω) are given by

$$S = \begin{pmatrix} 0 & 0 \\ G & 0 \end{pmatrix}$$
$$C_S = \begin{pmatrix} \overline{|c_1|^2} & \overline{c_1 c_2^*} \\ c_2 c_1^* & \overline{|c_2|^2} \end{pmatrix}.$$

The resulting noise wave correlation matrix of the global network is given by [1]

$$C_{\rm net} = \Lambda C_S \Lambda' + [I|\Lambda S] C_t [I|\Lambda S]'$$

where the dagger ($'$) indicates the Hermitian conjugate, the pipe symbol ($|$) designates the matrix augmentation. Λ is defined by

$$\Lambda = T_{ei}(I - ST_{ii})^{-1}$$

where subscript i designates waves shared at the internal connection between networks S and T, and subscript e designates the external waves at the scattering matrix terminals.

At f_o, the central frequency of the bandpass filter, the noise factor calculated using the noise wave formalism is then given by

$$F_1 = 1 + \left(\frac{\beta_1}{\alpha_1}\right)^2 \frac{\overline{|c_2|^2}}{\overline{|b_g|^2}} + \left(\frac{\beta_2 - \beta_1 G_o}{\alpha_1\alpha_2}\right)^2.$$

Referring to (1), F_1 can also be written as function of F_A

$$F_1 = 1 + \left(\frac{\beta_1}{\alpha_1}\right)^2 (F_A - 1) G_o^2 + \left(\frac{\beta_2 - \beta_1 G_o}{\alpha_1\alpha_2}\right)^2$$

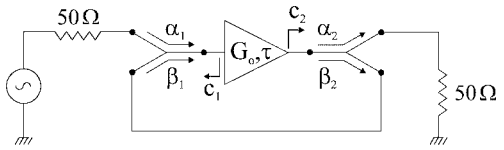

Fig. 8. Topology 2. Amplifier placed within the forward branch.

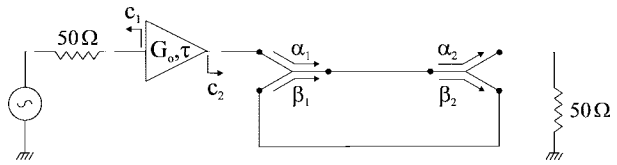

Fig. 9. Topology 3. Amplifier cascaded with a passive filter.

where b_g is the noise wave due to the source resistance at the input port of the filter with:

$$\overline{|b_g|^2} = kT.$$

2) Topology 2: Amplifier Placed Within the Forward Branch: The corresponding topology is given in Fig. 8. The scattering matrix and the noise correlation matrix of the amplifier are the same as for the topology 1, only the location of the amplifier has been changed within the filter structure. The transfer function $H_2(f)$ is given by

$$H_2(f) = \frac{G\alpha_1\alpha_2}{1 - G\beta_1\beta_2}.$$

Using the same method as for topology 1, the noise factor of this topology at f_o is given by

$$F_2 = 1 + \left(\frac{1}{G_o\alpha_1}\right)^2 \frac{\overline{|c_2|^2}}{\overline{|b_g|^2}} + \left(\frac{\beta_2 - \beta_1 G_o}{\alpha_1\alpha_2 G_o}\right)^2.$$

As it has been previously done for topology 1, F_2 can be expressed in terms of F_A as

$$F_2 = 1 + \frac{(F_A - 1)}{\alpha_1^2} + \left(\frac{\beta_2 - \beta_1 G_o}{\alpha_1\alpha_2 G_o}\right)^2.$$

3) Topology 3: Amplifier Cascaded with a Passive Filter: The last topology is given in Fig. 9. In this case, we choose to cascade the amplifier with a passive filter. The corresponding transfer function $H_3(f)$ is then given by

$$H_3(f) = \frac{G\alpha_1\alpha_2}{1 - \beta_1\beta_2 e^{-2j\pi f\tau}}.$$

To calculate F_3, we use the formula of Friis, and we obtain

$$F_3 = F_A + \frac{F_p - 1}{G_o} = F_A + \frac{1 - |H(f)|^2}{G_o|H(f)|^2}$$

with $F_p = (1/|H(f)|^2)$ the noise factor of the passive filter.

B. Minimum Noise Factor of the Three Topologies

To calculate the minimum noise factors of the three topologies, we first define the R and V parameters to set the filtering performances. These performances must not be modified by

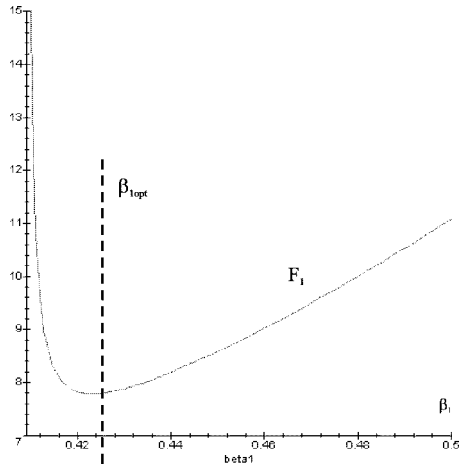

Fig. 10. Variation of F_1 as a function of β_1 in the case when $G_o = 2, V = 0.82$ $(R = 10), F_A = 9.3$ dB.

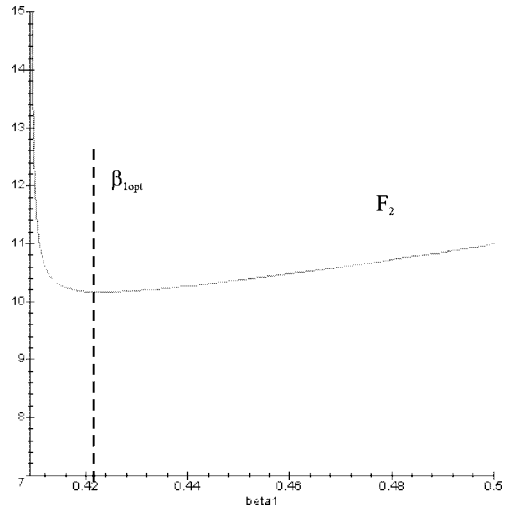

Fig. 11. Variation of F_2 as a function of β_1, in the case when $G_o = 2, V = 0.82$ $(R = 10), F_A = 9.3$ dB.

the improvement process of the noise factor and are defined considering the periodic property of the transfer function [3]

$$R = \frac{|S_{21}|_{\max}}{|S_{21}|_{\min}} = \frac{|S_{21}(f_0)|}{|S_{21}(f_0/2)|}$$

with

$$f_0 = 1/\tau$$

and

$$V = \frac{R-1}{R+1}. \tag{4}$$

In order to get the same filtering performances, the three topologies must be characterized by the same V and R parameters. With these parameters, two filters can be considered as equivalent even if they do not achieve the same gain at f_o. Indeed, the transfer function of the three topologies can be expressed as follows:

$$H_i(z) = \frac{K_i}{1 - Vz^{-1}}.$$

1) Minimum Noise Factor for Topology 1: In this case we have $V = \beta_1\beta_2 G_o \Rightarrow \beta_1 = V/(\beta_2 G_o)$ and $\beta_2 = V/(\beta_1 G_o)$. This leads to $V/G_o < \beta_{1,2} < 1$ with $V < 1$ [see (4)] and $G_o > 1$. Then, the higher G_o is, the more important the range of the values of β is. For lossless couplers, we assume that $\alpha_1^2 + \beta_1^2 = 1$, $\alpha_2^2 + \beta_2^2 = 1$, and $\beta_1\beta_2 = V/G_o$. We then can find an expression of F_1 as a function of V, β_1, G_o, and F_A. An analytical study leads to determine the expression of $\beta_{1\text{opt}}$, for which we obtain the minimal noise factor. An example is given in Fig. 10 for typical values of G_0, V, and F_A derived from Section III. We can then deduce $\beta_2 = V/(\beta_1 G_o)$, α_1, and α_2. After the substitution of the value of $\beta_{1\text{opt}}$ in F_1, we now study the variation of F_1 as a function of G_o. It can be shown that F_1 decreases when G_o increases. So the limit value of F_1, when F_A is kept constant, is given by

$$\lim_{G_o \to \infty} F_1 = 1 + V^2(F_A + 1) - 2V + 2V\sqrt{F_A}(1 - V)$$

and

$$\lim_{G_o \to \infty} < F_A.$$

The fact that F_A is kept constant while G_0 varies is particularly interesting in the case where we can choose between two amplifiers of the same noise factor but of different gain values. In this case the highest gain must be taken. Moreover, it can be demonstrated that $F_{1\,\lim} < F_A$. Indeed

$$\frac{d(F_{1\,\lim} - F_A)}{dF_A} = \frac{V^2(\sqrt{F_A} - 1) + V - \sqrt{F_A}}{\sqrt{F_A}}.$$

This expression is equal to zero when F_A is equal to $F_{Ao} = (V^2/(1+V)^2)$. As $V < 1$ we obtain $F_{Ao} < 1$ which is nonphysical. So $d(F_{1\,\lim} - F_A)/dF_A$ always keeps the same sign for all values of $F_A \geq 1$. For $F_A = 1$ we have

$$\frac{d(F_{1\,\lim} - F_A)}{dF_A} = (V - 1) < 0$$

and

$$F_{1\,\lim} - F_A|_{F_A=1} = 0 \Rightarrow F_{1\,\lim} < F_A.$$

With this topology, we are in the case where we can obtain, at the resonance frequency f_o, a noise factor of the filter lower than the one of the amplifier used.

2) Minimum Noise Factor for Topology 2: With the same method, we now calculate F_2 as a function of V, β_1, G_o, and F_A. Afterwards, we evaluate $dF_2/d\beta_1$ to find $\beta_{1\text{opt}}$. We derive in this case that the expression of $\beta_{1\text{opt}}$ is the same as for topology 1. An example of $F_2 = f(\beta_1)$ is given in Fig. 11 with the same values for V, G_o, and F_A as for topology 1. The only difference is that $lim_{G_o \to \infty} F_2 = F_A$, and consequently, F_2 cannot be less than the noise factor of the amplifier.

3) Minimum Noise Factor for Topology 3: In this case, $V = \beta_1\beta_2 \Rightarrow \beta_1 = V/\beta_2$ and $\beta_2 = V/\beta_1$. So $V < \beta_{(1,2} < 1$ with $V < 1$ and $G_o > 1$. To minimize F_3 we look for the minimum of F_P, the noise factor of the passive part (see Section III-A.3) with

$$F_3 = F_A + \frac{F_p - 1}{G_o}.$$

We know that $\alpha_1^2 + \beta_1^2 = 1$, $\alpha_2^2 + \beta_2^2 = 1$, and $V = \beta_1\beta_2$. We then can find the expression of F_P as a function of V and

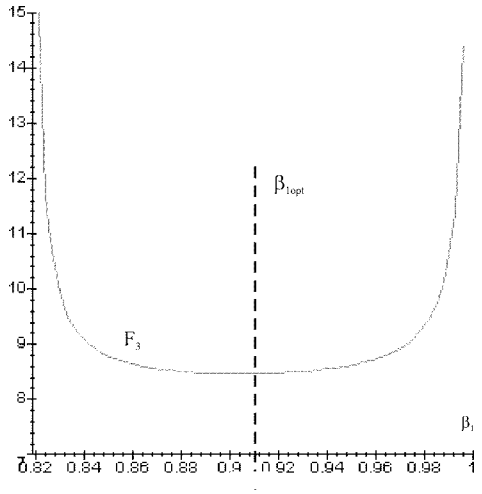

Fig. 12. Variation of F_3 as a function of β_1, in this case when $G_o = 2, V = 0.82, F_A = 9.3$ dB.

β_1 and calculate $dF_3/d\beta_1$ to find $\beta_{1\text{opt}}$. We obtain $\beta_{1\text{opt}}\sqrt{V}$. An example of $F_3 = f(\beta_1)$ is derived in Fig. 12.

We also find $\beta_{2\text{opt}} = (V/\beta_{1\text{opt}}) = \sqrt{V} = \beta_{1\text{opt}}$, F_P is minimum when the couplers are identical. Moreover, for this topology, $\lim_{G_o\to\infty} F_3 = F_A$, leading to the same conclusion as for topology 2.

C. Comparison of the Three Topologies

To compare the topologies, we consider that the same amplifier is used with the same noise factor and gain values and we also consider that the three topologies are optimum in terms of noise ($\beta_1 = \beta_{1\text{opt}}$) and achieve the same filtering performance V.

We know that

$$\begin{cases} \lim\limits_{G_o\to\infty} F_1 < F_A \\ \lim\limits_{G_o\to\infty} F_2 = F_A \\ \lim\limits_{G_o\to\infty} F_3 = F_A. \end{cases}$$

It can be analytically derived, thanks to the software Maple V [5] that

$$\begin{cases} F_3 < F_1 < F_2 & \text{if} \quad 1 < G_o < G_{\text{lim}} \\ F_1 < F_3 < F_2 & \text{if} \quad G_o > G_{\text{lim}} \end{cases}$$

with

$$G_{\text{lim}} = \frac{V}{(1-V)}\sqrt{\frac{F_A(V+1)+(1-V)+2\sqrt{F_A}}{F_A(V+1)^2-(V-1)^2}}$$

for which $F_3 = F_1 = F_2$ at f_o.

We can then say that topology 2 is the worst topology for noise and that the choice between topology 1 and 3 depends on V and the gain G_o of the amplifier. Besides, an important advantage of topology 1 is that this topology is the most interesting with regard to power handling behavior. Indeed, the amplifier is placed within the feedback branch and sees at its input less power than when connected directly at the input of topology 3. Moreover, better selectivity can be achieved thanks to the gain value within the loop which is not possible for topology 3 with the limitation inherent to the couplers gaps. Therefore, topology 1 can be considered as the best solution for our problem.

TABLE I
$G_o > G_{\text{lim}} \Rightarrow F_1 < F_3 < F_2$ AT f_o

	β_{1opt} (dB)	β_2 (dB)	F(f_o) (dB)	simulated results
topology 1	-5.12	-0.76	8.46	
topology 2	-5.12	-0.76	10.75	figure 13
topology 3	-1.76	-1.76	9.28	

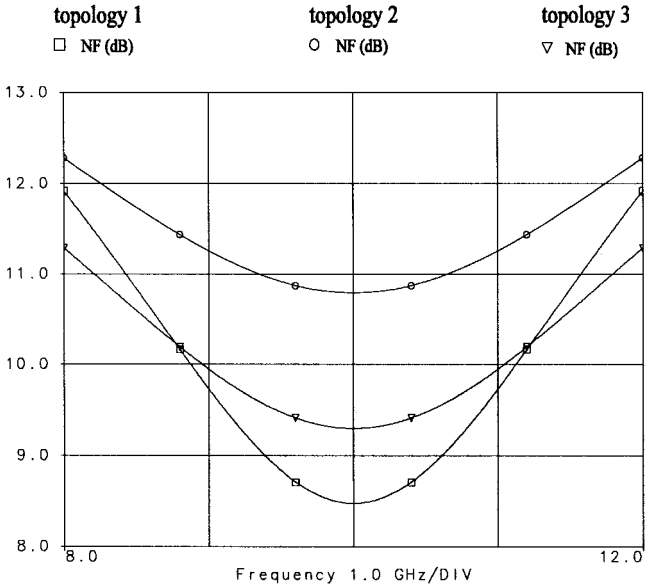

Fig. 13. Simulated noise figures for example 1: $G_o > G_{\text{lim}}$ ($F_1 < F_3 < F_2$ at f_o).

D. Validation Examples

Using the microwave CAD software HP-EEsof,[1] we present three examples to validate our calculations. The elements of the circuits used are all ideal elements. The following tables represents the different values of coupling $\beta_{1\text{opt}}$ calculated to obtain the minimum noise factor for each topology.

1) Example 1: $G_o = 1.316$, $F_A = 9.3$ *dB*, $R = 5$ ($V = 2/3$), $G_{\text{lim}} = 1.2$, $G_o > G_{\text{lim}}$: The values of G_o, F_A, and R correspond to the ones used in the filters of Section III already realized using MMIC technology [3]. These filters were built using topology 1 with 3-dB couplers at the input and output ports (see Fig. 5). The measured noise factor was 11.7 dB (see Fig. 6) at f_o. We notice in Table I that the optimum noise factor decreases down to 8.47 dB less than F_A for topology 1, while staying greater than F_A for topologies 2 and 3 (see Fig. 13).

As it has been demonstrated before, when $G_0 > G_{\text{lim}}, F_1 < F_3 < F_2$ at f_0.

[1] HP-EEsof, Libra reference manual.

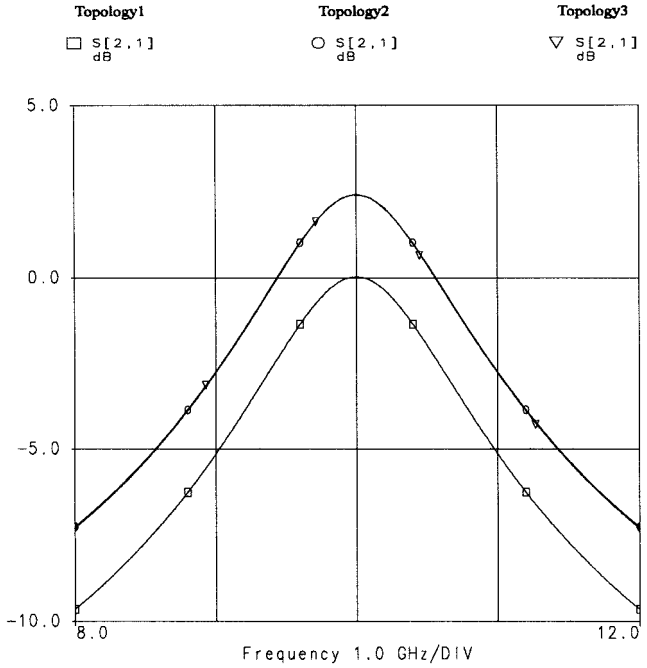

Fig. 14. Simulated response for example 1.

TABLE II
$G_o < G_{\lim}$ $(F_3 < F_1 < F_2)$

	β_{1opt} (dB)	β_2 (dB)	F(f_o) (dB)	simulated results
topology 1	-3.88	-0.25	10.2	
topology 2	-3.88	-0.25	11.44	figure 15
topology 3	-0.87	-0.87	9.35	

Fig. 14 presents the corresponding transfer function for the three topologies. These transfer functions are obviously equivalent in terms of selectivity.

2) Example 2: $G_o = 1.316$, $F_A = 9.3$ *dB*, $R = 10$ $(V = 0.82)$, $G_{\lim} = 1.8$, $G_o < G_{\lim}$*:* We now try to build more selective filters with the same amplifier. We set $R = 10$ $(V = 0.82)$, and in this case $G_o < G_{\lim}$. This leads to $F_3 < F_1 < F_2$ (see Table II).

With examples 1 and 2, using the same amplifier, we notice that the noise factor increases when the selectivity increases. This is verified for the three topologies (see Fig. 15).

3) Example 3: $G_o = 2, F_A = 9.3$ *dB*, $R = 10$ $(V = 0.82)$, $G_{\lim} = 1.8$, $G_o > G_{\lim}$*:* In this case, we keep $R = 10$ but we increase the gain $(G_o = 2)$, which leads to $G_o > G_{\lim}$. This shows that if the gain is increased (for the same F_A) the noise factor of the filter decreases as expected (see Table III).

As expected, we find that, when $G_o > G_{\lim}$, F_1 becomes less than F_3 (see Fig. 16).

E. Experimental Low Noise Active Recursive Filter Design

To experimentally validate our approach, we present the design of a first-order recursive filter using topology 1 in

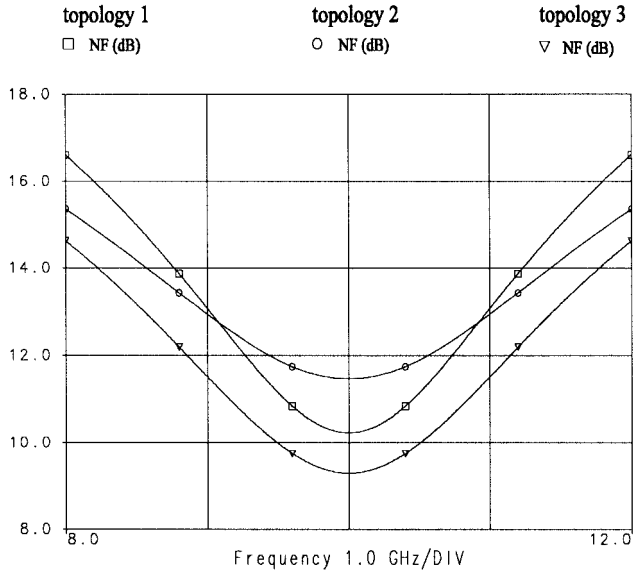

Fig. 15. Simulated noise figures for example 2: $G_o < G_{\lim}$ $(F_3 < F_1 < F_2$ at $f_o)$.

TABLE III
$G_o > G_{\lim}$ $(F_1 < F_3 < F_2)$

	β_{1opt} (dB)	β_2 (dB)	F(f_o) (dB)	simulated results
topology 1	-7.47	-0.29	8.91	
topology 2	-7.47	-0.29	10.07	figure 16
topology 3	-0.87	-0.87	9.28	

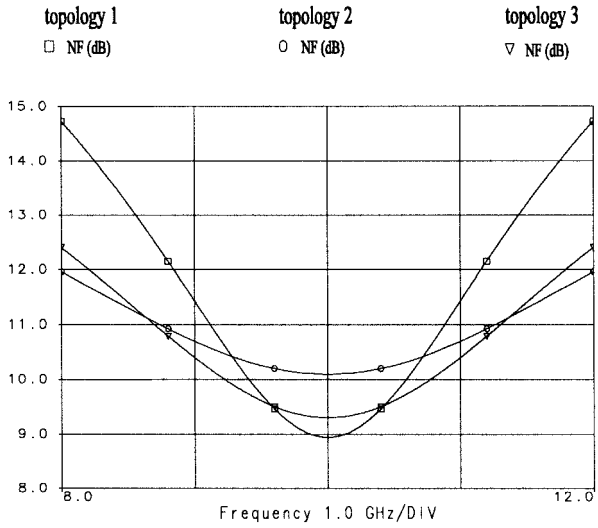

Fig. 16. Simulated noise figures for example 3: $G_o > G_{\lim}$ $(F_1 < F_3 < F_2$ at $f_o)$.

MMIC technology (Philips microwave ED02AH process).[2] This filter, whose layout is given in Fig. 17, has the same filtering performances as the one presented in Section III. Couplings and gain values are chosen to obtain the lowest noise factor according to the analysis presented. We note

[2] Philips microwave, ED02AH design manual.

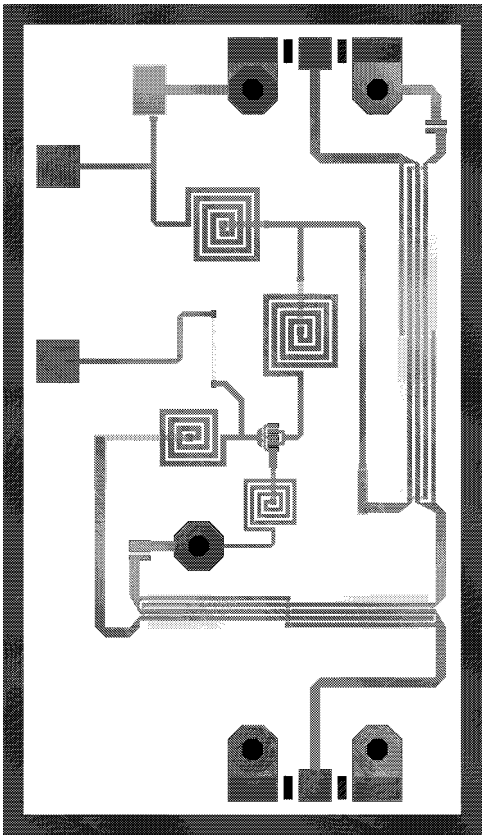

Fig. 17. Layout of the low-noise first-order active recursive filter.

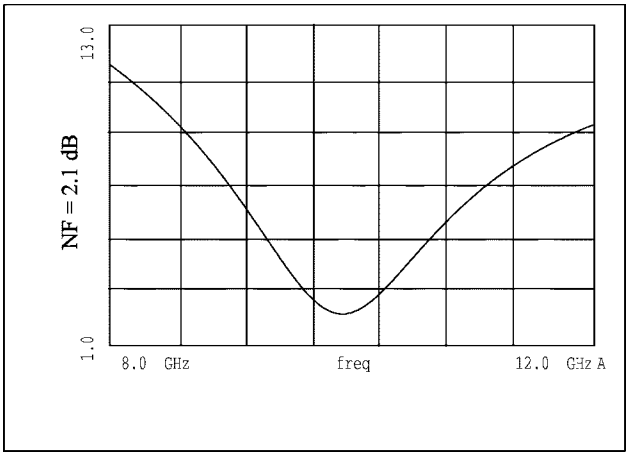

Fig. 18. Simulation results of the low-noise first-order active recursive filter.

that the noise figure is now equal to 2.1 dB (see Fig. 18) as compared to the initial 11.7 dB (see Fig. 6).

IV. $\lambda/2$ Microstrip Planar Filters [6]

A. Theatrical Background

The filter is constituted with a $\lambda/2$ microstrip planar resonator whose losses are compensated by an active feedback loop as shown in Fig. 19. S_1, S_2, and S_3 are the coupled lines gaps. In order to simplify the theoretical analysis of this circuit, we use the corresponding lumped element equivalent circuit shown in Fig. 20.

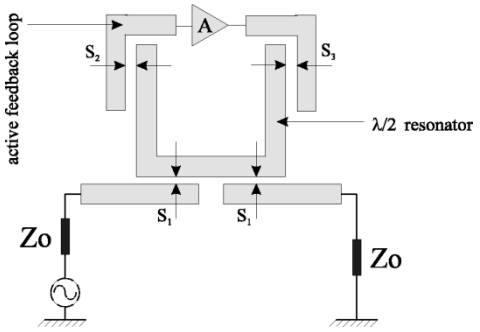

Fig. 19. Real schematic of active filter using a feedback amplifier-based loop.

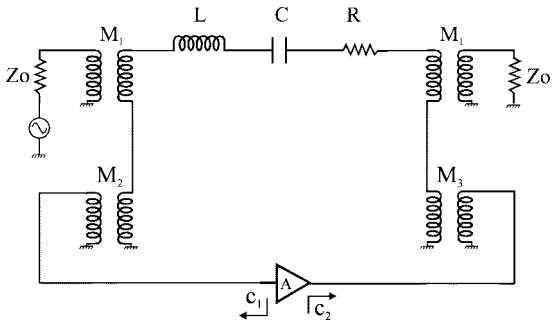

Fig. 20. Electrical equivalent circuit of the active filter using a feedback amplifier-based loop.

In this schematic, c_1 and c_2 are the noise waves due to the amplifier. Resistance R, self-inductance L, and capacitance C correspond to the $\lambda/2$ passive resonator. The M_i elements ($i = 1, 2, 3$) are mutual inductances. M_1 simulates the couplings between the resonator and the filter input and output ports while M_2 and M_3 simulate the coupling between the resonator and the unilateral amplifier block A matched to 50 Ω. The noise factor obtained using the noise wave formalism can then be put into the following form:

$$F = F_P + \frac{1}{|b_g|^2 M_1^2} \left|(M_2 + M_3 G)\overline{c_1} - M_3 \overline{c_2}\right|^2 \qquad (5)$$

where $F_P = 1 + (RZ_o/\omega_o^2 M_1^2)$ is the noise figure of the passive filter, and b_g is the noise wave due to the source impedance Z_0 at the input port of the filter.

We can now minimize the noise factor in (5) by choosing M_2 and M_3 to satisfy the following condition:

$$M_2 + M_3 G = 0. \qquad (6)$$

By substituting (6) into (5), the optimum noise factor of the filter can be expressed as

$$F_{\text{opt}} = F_P + \frac{M_e^2 |\overline{c_2}|^2}{M_1^2 |\overline{b_g}|^2}.$$

We can also express F_{opt} as a function of F_A

$$F_{\text{opt}} = F_P + \frac{M_3^2}{M_1^2} (F_A - 1)|G|^2.$$

TABLE IV
EXAMPLES USING EQUIVALENT CIRCUIT

	M_1 (nH)	M_2 (nH)	M_3 (nH)	NF (dB)
M_2=-M_3G	0.2	0.21	0.07	2.28
M_2#-M_3G	0.2	0.09	0.24	4.63

TABLE V
EXAMPLES USING REAL CIRCUIT

	S_1 (mm)	S_2 (mm)	S_3 (mm)	NF (dB)
M_2=-M_3G	0.1	0.05	0.8	2.2
M_2#-M_3G	0.1	0.45	0.05	10.5

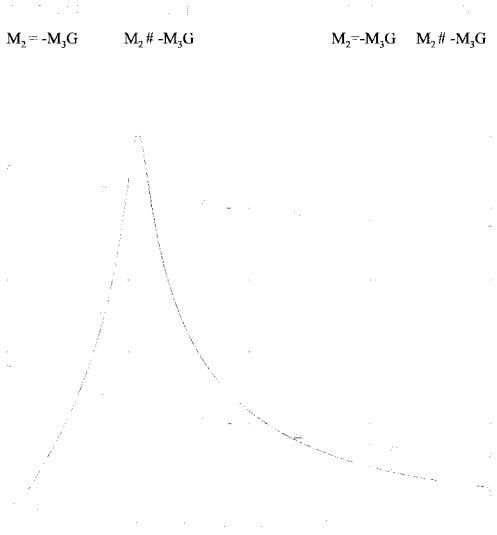

Fig. 21. Equivalent circuit. Noise figure is minimum when $M_2 = -M_3G$.

To validate our approach, we present simulations of four different examples, the two first (see Table IV) using the filter equivalent circuit ($L = 1.65$ nH, $C = 1.22$ pF, $R = 0.2\ \Omega$) and the others using real microstrip elements (see Table V).

The corresponding simulation results for the equivalent circuit and real circuit are given in Figs. 21 and 22, respectively.

Note in Figs. 21 and 22 that the process of minimizing the noise factors of the filters is done while keeping the same filtering performances (the same S_{21} response), thus validating our approach.

B. Experimental Results

This active filter has been implemented on a 0.17-mm-thick Duroid substrate ($\varepsilon_r = 2.43$). The amplifier employed here is a Mitsubishi FET transistor MGFC1423. Figs. 23 and 24 presents simulated and measured S_{21}, S_{11} and noise figure of the filter. We notice that the measured noise figure at f_o has been lowered to 4.5 dB using our approach.

Note the good agreement between theoretical and experimental results.

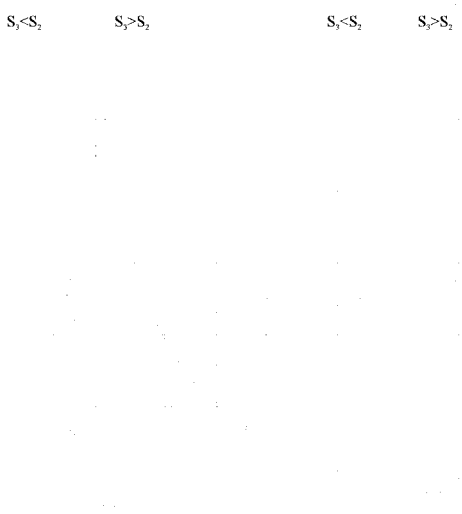

Fig. 22. Real circuit. Noise figure is minimum when $S_2 < S_3$.

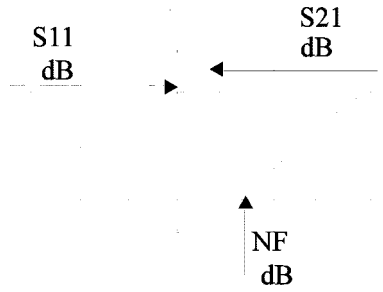

Fig. 23. Simulated results of planar active filter.

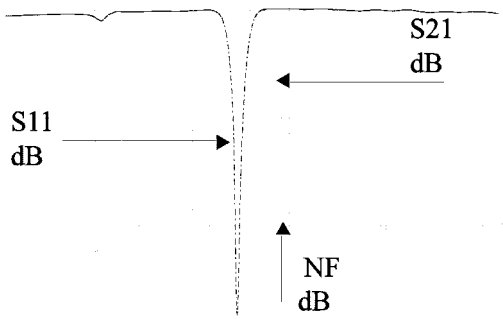

Fig. 24. Experimental results of planar active filter.

V. Conclusion

In this paper, we have analytically demonstrated, numerically and practically verified, using a noise wave technique, that noise figures of various active filters can be efficiently minimized.

In the first case, we have analytically analyzed three different topologies of first-order microwave active recursive filters using the same amplifier. We have derived the analytical expressions of the noise factor for each topology and validated our results with the measurement of a MMIC recursive chip. We have also shown, for each topology, the existence of optimal coupling values, for which we achieve minimum noise factors.

The most important result is that, with the first of the three topologies, when the amplifier is placed in the feedback branch, the noise factor of the filter could even be less than the one of the amplifier used. This result shows that recursive structures are a promising solution to low noise filtering problems, even better than the classical cascade of a low-noise amplifier with a passive filter structure. We have also studied the influence of the value of the gain upon the noise factor of the three topologies and validated our analysis and results with different simulated examples. This has led to the design of a low noise recursive chip for which the noise factor has been optimally lowered.

In the second case, we have studied $\lambda/2$ microstrip resonator filters. Our analyses lead us to conclude that the appropriate choice of the coupling values between the amplifier line section and the resonators could achieve a low-noise filter when using an amplifier-based loop. We have validated our approach with simulated and measured results of the optimal filter topology.

References

[1] S. Wedge and D. Rutledge, "Wave techniques for noise modeling and measurement," *IEEE Trans. Microwave Theory Tech.*, vol. 40, pp. 2004–2012, Nov. 1992.

[2] S. E. Sussman-Fort, "Design concepts for microwave AsGa FET active filters," *IEEE Trans. Microwave Theory Tech.*, vol. 37, pp. 1418–1424, Sept. 1989.

[3] M. Delmond, L. Billonnet, B. Jarry, and P. Guillon, "Hybrid and monolithic tunable recursive filter design at microwaves including a new stability analysis procedure," *Microwave Opt. Technol. Lett.*, vol. 10, pp. 263–270, Dec. 1995.

[4] M. Delmond, L. Billonnet, B. Jarry, and P. Guillon, "New design approach for high-order active recursive filter using MMIC technology," in *EuMC'96, 26th European Microwave Conf. Proc.*, Prague, vol. 1, Sept. 1996, pp. 405–408.

[5] V. Maple, *Reference Manual, Waterloo Maple Software*, 1993.

[6] C. Cenac *et al.*, "X-band active filters with half-wave or ring resonators and variable gain and phase monolithic circuits," *Microwave Opt. Technol. Lett.*, Apr. 1996.

Hilal Ezzedine was born in Lebanon. He received the "DEA d'Electronique" from the University of Limoges, France, in 1996. Since 1996 he has been working toward the Ph.D. degree in electronics at the "Institut de Recherche en Communications Optiques et Microondes," in Limoges.

His principal research interest is the study of the noise in the microwave active filters.

Laurent Billonnet was born in Beaumont-Sur-Oise, France, in May 1966. He received the doctorat degree from the University of Limoges in 1993.

Currently, he is an Assistant Professor at the University of Limoges, working at the Microwaves and Optical Communications Research Institute. His main field of interest is the microwave filtering functions. He is currently involved in the study of recursive and transversal structures, analog phase shifters, NIC's, and their applications at microwaves.

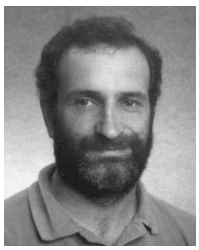

Bernard Jarry (M'93–SM'97) received the Ph.D. degree and HDR from the University of Limoges, France, in 1985 and 1994, respectively.

In 1986, he joined Thomson-CSF (Orsay, France) working on monolithic W-band mixers. Since 1987, he has been at the University of Limoges, where he is currently Assistant Professor. At the Microwaves and Optical Communications Research Institute (URA CNRS), his research interests are in the fields of microwave passive and active filters, low noise devices, signal generation, and frequency control circuits.

Pierre Guillon (SM'92) was born in May 1947. He received the Doctorat es Sciences degree from the University of Limoges, France, in 1978.

From 1971 to 1980, he was with the Microwave and Optical Communications Laboratory, University of Limoges, where he studied dielectric resonators and their applications to microwave and millimeter-wave circuits. From 1981 to 1985, he vas a Professor of Electrical Engineering at the University of Poitiers, France. In 1985, he joined again the University of Limoges, where he is currently a Professor and a head of a research group in the area of microwave and millimeter-wave devices.